

## INTEGRATION OF SPECTRAL AND TEXTURAL FEATURES FROM IKONOS IMAGE TO CLASSIFY VEGETATION COVER IN MOUNTAINOUS AREA

*(Integrasi Fitur Spektral dan Tekstur dari Citra IKONOS untuk  
Klasifikasi Tutupan Vegetasi di Daerah Pegunungan)*

KETUT WIKANTIKA<sup>1)</sup>

### ABSTRAK

*Studi ini mengevaluasi penggunaan fitur spektral dan tekstur secara terintegrasi yang didapat dari citra IKONOS untuk mengidentifikasi tipe-tipe tutupan lahan pertanian di daerah pegunungan. Studi meliputi pra pengolahan citra, pengembangan metode kuantisasi citra, penghitungan nilai tekstur, pembuatan dataset dan penilaian akurasi. Pra pengolahan citra berfokus pada registrasi citra dan normalisasi topografis. Dalam studi ini dikembangkan dua metode kuantisasi citra yaitu segmentasi citra dan filter rata-rata. Segmentasi citra mengklasifikasi citra kedalam beberapa segmentasi berdasarkan determinasi jumlah total piksel setiap kelas, sedangkan filter rata-rata mengelompokkan citra berdasarkan rata-rata nilai angka digital dalam ukuran window tertentu. Empat ukuran tekstur yaitu inverse difference moment, contrast, entropy dan energy dihitung dengan grey level co-occurrence matrix (GLCM). Hasil studi menunjukkan kombinasi aspek spektral dan tekstur meningkatkan akurasi klasifikasi secara signifikan dibandingkan klasifikasi hanya menggunakan fitur spektral saja. Segmentasi citra dan filter rata-rata dapat memberikan bentuk-bentuk spasial tipe tutupan lahan pertanian yang lebih efektif dibanding menggunakan citra dengan derajat keabuan 256. Ketelitian keseluruhan meningkat 11,33% ketika menggunakan integrasi spektral dan fitur tekstur inverse difference moment (5x5) dan energy (9x9).*

Keywords ; spectral, texture, IKONOS image, vegetation cover, image segmentation, averaging filtered.

### INTRODUCTION

Texture is an important characteristic for the analysis of many types of images such an image obtained from aircraft or satellite platforms. It is the visual effect, which is produced by spatial distribution of tonal variations over relatively small areas (Baraldi and Parmiggirani, 1995). The concept of texture can be investigated through its relationship

---

<sup>1)</sup>Scientist on Expertise Group on Remote Sensing and Geographical Information Science Faculty of Civil Engineering and Environment; Center for Remote Sensing Institute of Technology Bandung (ITB) Jln. Ganesha 10, Bandung 40132, Indonesia e-mail: [ketut@crs.itb.ac.id](mailto:ketut@crs.itb.ac.id)

with spectral; in fact, textural and spectral information can both be present in an image or either one can dominate the other.

Many researches have investigated on extraction of textural features for mapping urban environment and land use classification using neural network (Bardibas, 1998), several filtering methods (Beauchemin *et.al.*, 1993; Dutra and Nelseon, 1984; Sabhan and Dikshit, 1999a & 1999b; Toll, 1985 and Zhang, 1999), local standard deviation and autocorrelation (Horgan *et.al.*, 1992), principal component and filtering (Kuplich, Freistas and Soares, 2000), multitemporal SAR data (Kurosu *et.al.*, 1999), morphological processing (Karathanassi, Iossifidis, Rokos, 2000; Smits *et. al.*, 1998), and image segmentation (Conner, Trivedi, Harlow, 1984; Kurosu *et. al.* 1999; Ryherd and Woodcock, 1996). Their studies show that the integration of spectral and texture features improve the classification accuracy result.

The objective of this study is to clarify the role of integration of spectral and textural features derived from IKONOS image for classification of vegetation cover types in mountainous area with a case study in Pangalengan area, West Java, Indonesia. Two image quantization methods were developed to calculate textural features. Four textural measures, i.e., inverse difference moment, contrast, entropy and energy were applied based on grey level co-occurrence matrix (GLCM). The maximum likelihood classification algorithm was used to classify land cover types of the study area and finally more than 280 data sets were assessed.

### **Study site**

This study was conducted in part of one of villages in Pangalengan sub-district, Margamekar village, in the south of Bandung, West Java, Indonesia, roughly between longitudes  $107^{\circ} 25' - 107^{\circ} 40'$  E and latitudes  $7^{\circ} 5' - 7^{\circ} 20'$  S measuring approximately  $13.45 \text{ km}^2$ . The climate at study area is humid tropical with annual precipitation averaging 1250 mm every year (Data Monografi Kecamatan, 2001). Generally, the highest rainfall consistently occurs between December and March, and the lowest rainfall occurs between July and August. The topography is generally classified into three classes; flat to mildly undulating (29%), undulating to hilly (33%) and hilly to mountainous (38%). Elevation varies from 1365 m to 1550 m above mean sea level. The major land cover types are residential, lake water, fallow land, vegetables and tea plantation. Cabbage, potato and tomato are dominant vegetable types of the study area, while tea plantation covers more than 30% of the total size of the study area.

### **Data**

IKONOS satellite image is a main data used in the study. Table 1 shows the specification of the data. Other data are digital elevation model (DEM) with grid size of 50 m collected for pre processing and other image analysis.

Table 1. IKONOS data specifications

Sensor	Spectral bands	Other specifications
IKONOS	Band-1/Blue: 0.45-0.52 $\mu\text{m}$ Band-2/Green: 0.52-0.60 $\mu\text{m}$ Band-3/Red: 0.63-0.69 $\mu\text{m}$ Band-4/NIR: 0.76-0.90 $\mu\text{m}$	Spatial resolution: 4 m Sun azimuth: 108.66° Sun elevation: 56.57° Overpass time: ~10:30 am Acquired on February 6, 2000 Processing level: Geo product

## METHODS

### Pre processing data

Pre processing image focuses on geometric correction and topographic normalization. The IKONOS image was projected onto universal transverse mercator (UTM) with WGS 84 datum corresponding to other geographic data such as administrative boundary and DEM data. Topographic slope may introduce radiometric distortion of the recorded signal. In some locations, the area of interest might even be in complete shadow, dramatically affecting the brightness values of the pixels involved (i.e spectral reflectance) (Colby, 1991). Therefore it is important to reduce or remove topographic effects, especially in mountainous area. In this study, the study area was assumed as a lambertian reflectance model, it means that the surface reflected incident solar energy uniformly in all directions, and that variations in reflectance were due to the amount of incident radiation. To minimize the effect of illumination differences on the surface reflectance in mountainous areas, digital number of spectral bands was calibrated using normalized brightness equation (Jensen, 1996). This equation needed the information of sun azimuth and elevation at the time of image acquisition, DEM and original image.

### Spectral reflectance measurement

In this study, characteristics of spectral reflectance of land cover such as canopies of different vegetables, tea plantation and fallow land were measured using portable photometer type 2703. The objective of this work is to select appropriate spectral band of IKONOS image for textural extraction. The spectral interval of photometer is 25 nm (400 to 675), 50 nm (700 to 750) and 100 nm (750 to 1050). Several measurements were conducted in which each observation was measured twice and then the average observation was calculated. All measurements were carried out in day time under clear atmospheric condition. Figure 1 shows characteristics of spectral reflectance profiles for tomato, long chili, tea plantation, fallow land, cabbage and potato. In this case, the coverage condition of fallow land shows no vegetation cover on its surface.

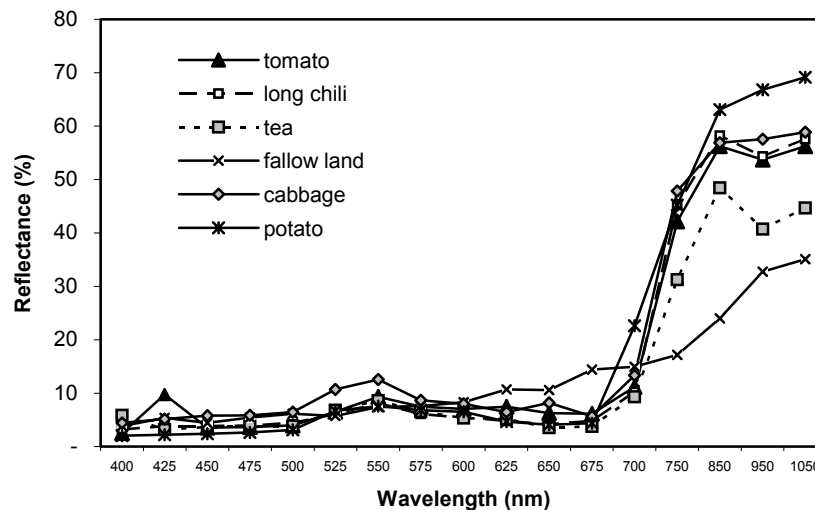


Fig 1. Land cover spectral reflectance profiles measured by sun photometer portable

According to the spectral reflectance profiles in Figure 1, tomato, long chili, cabbage and potato were classified into united vegetable class. The spectral reflectance values of this class was fairly low ranging from 0 to 10% in the visible region. These spectral reflectance profiles correspond to spectral signatures extracted from corrected IKONOS image.

### Image quantization

The number of grey level is an important factor in the computation of GLCM. Therefore, in this study, commonly used method of image quantization, stored in a 256 grey level, and a proposed image quantization method; image segmentation and averaging filtered, were applied. Image segmentation method classifies the image into several segmentations based on determination of total number of pixels per class, while averaging filtered classifies the image based on the average of digital number values within a window size.

### GLCM and textural measures

Commonly used method to calculate textural information is based on GLCM (grey level co-occurrence matrix). The definition of GLCM's is as follows (Haralick, Shanmugam and Dinstein, 1973; Bandibas, 1998). Suppose an image to be analyzed is rectangular and has  $N_x$  resolution cells in the horizontal direction and  $N_y$  resolution cells in the vertical direction (Baraldi and Parmiggiani, 1995). Suppose that the grey tone appearing in each resolution cell is quantized to  $N_g$  levels (Beauchemin, Thomson and Edwards, 1996). Let  $L_x = \{1, 2, \dots, N_x\}$  be the horizontal spatial domain,  $L_y = \{1, 2, \dots,$

$N_y$  be the vertical spatial domain, and  $G = \{1, 2, \dots, N_g\}$  be the set of  $N_g$  quantized grey tones. The set  $L_y \times L_x$  is the set of resolution cells of the image ordered by their row-column designations (Colby, 1991). The image  $I$  can be represented as a function, which assigns some grey tones in  $G$  to each resolution cell or pair of coordinates in  $L_y \times L_x$ ;  $I: L_y \times L_x \rightarrow G$ . The texture-context information is specified by the matrix of relative frequencies  $P_{ij}$  with two neighboring pixels separated by distance  $d$  occur on the image, one with gray level  $i$  and the other with gray level  $j$ .

Four texture measures were applied; inverse difference moment, contrast, entropy and energy (Baraldi and Parmiggiani, 1995; Karathanasi; Iossifidis and Rokos, 2000; Kuplich, Freitas, Soares, 2000; Kurosu *et.al.*, 1999; Marceau *et.al.*, 1990; Soares *et.al.*, 1997; Soh and Tsatsoulis, 1999; Zhang, 1999). Inverse difference moment which is also called as homogeneity is calculated using the following equation:

$$\text{Inverse difference moment} = \sum_{i=1}^{N_g} \sum_{j=1}^{N_g} \frac{1}{1 + (i - j)^2} P(i, j) \dots\dots\dots(1)$$

The contrast which measures is the difference between the highest and the lowest values of a continuous set of pixels is calculated using the following equation:

$$\text{Contrast} = \sum_{i=1}^{N_g} \sum_{j=1}^{N_g} (i - j)^2 P(i, j) \dots\dots\dots(2)$$

The entropy measures the disorder of an image. When the image is not texturally uniform, entropy is very large. Entropy is calculated using the following equation:

$$\text{Entropy} = - \sum_{i=1}^{N_g} \sum_{j=1}^{N_g} P(i, j) \log(P(i, j)) \dots\dots\dots(3)$$

The energy is also called the angular second moment or uniformity. Energy is calculated using the following equation:

$$\text{Energy} = \sum_{i=1}^{N_g} \sum_{j=1}^{N_g} (P(i, j))^2 \dots\dots\dots(4)$$

In this study, twelve window sizes of 3x3, 5x5, 7x7, ... 21x21, 23x23, 25x25 pixels were examined. The interpixel distance in the co-occurrence matrix calculation was one and the average of the four main interpixel angles was used for the computations. The textural features were obtained by using NIR band of IKONOS image. The reason for choosing this band for textural analysis was due to the fact that this band had maximum variability in terms of standard deviation and range of grey level values compared with other bands. In addition NIR, band is useful for determining vegetation types, vigor and biomass content, and delineating water bodies (Lillesand and Kiefer, 1994). These characteristics can be beneficial to classify the land cover types over the study area.

## RESULTS AND DISCUSSION

Figure 2 shows a portion of the study area in a 256 grey level (A), segmented into four classes (B) and eight classes (C), and averaging filtered using window sizes of 3x3, 5x5, 7x7 (D, E, F), respectively. Fallow land, which is indicated by area with white border, was classified into the same segment with water feature, in case of B. But the performance of the segment class was different when the whole image segmented into eight classes (C), where the fallow land consists of two segments, i.e, segment with grey level values of 0-39 and 40-58. The grey level value of the whole image was averaged using window sizes of 3x3, 5x5 and 7x7 pixels as shown in figure 4D, E, and F, respectively. The figures show that the performance of the spectral visualization is different each other.



Fig 2. Input images for textural features calculation: (A). A 256 grey level, (B). Image segmentation in four classes, (C). Image segmentation in eight classes, (D). Averaging filtered with 3x3 pixels, (E). Averaging filtered with 5x5 pixels, (F). Averaging filtered with 7x7 pixels.

There were calculated 288 textural features. The 355 data sets were made, consisting of one data set developed only using spectral bands 1, 2, 3, and 4 of IKONOS image, 288 data sets were developed using combination of single textural feature and all bands, and 66 data sets were developed using combination of multiple textural features and all bands. All data sets were used to classify land cover into five classes, i.e. water, fallow land, vegetable field, tea plantation and residential areas using maximum likelihood classification algorithm (Lillesand and Kiefer, 1994). Accuracy assessment was conducted to compare the classification result with the reference data. It can be quantitative with the purpose of identifying and measurement of map errors (Lillesand and Kiefer, 1994). It has been shown that more than 250 reference pixels are required to estimate the accuracy of a class within plus or minus five percent (Congalton, 1999). In this study, four hundred reference pixels were collected to assess the accuracy of land cover classes over the study area.

The overall classification accuracy of pure spectral bands of IKONOS was 79.75% (Table 2). Table 3 Summarizes the overall classification accuracies using the combination of spectral and single textural features derived from IKONOS. This Table 3 indicates that the combination between the spectral and single textural features gives a better accuracy than using only the spectral images. Quantization image with averaging filtered of 7x7 pixels provides better overall classification accuracy than the others, having accuracy ranges from 88% to 90%. The use of entropy in all window sizes and spectral features improve the overall classification accuracies than using spectral only. The overall classification accuracies with window size of larger than 15x15 do not improve significantly for contrast (a 256 grey level, segmentation in 8 classes, averaging filtered with window size of 7x7), entropy (segmentation in 8 classes), energy (segmentation in four and eight classes). For residential class, which is relatively heterogeneous than other classes, has the optimal window size of 3x3 pixels. While tea class has the optimal window size from 3x3 to 15x15 pixels.

Table 2. The error matrix of classification result using spectral feature only

Classified as	Reference data					Total
	Water	Fallow	Tea	Vegetable	Residential	
Water	<b>15</b>	1	1	1	0	18
Fallow	1	<b>67</b>	2	10	10	90
Tea	0	2	<b>55</b>	10	1	68
Vegetable	1	6	3	<b>124</b>	13	147
Residential	2	6	2	9	<b>58</b>	77
<b>Total</b>	19	82	63	154	82	<b>400</b>

The overall accuracy is calculated with  $15+67+55+124+58/400=79.75\%$

Table 3. The overall accuracy (%) using single texture feature

No	Texture Window size	Image quantization method					
		the 256 grey level	Segmentation		Averaging filtered		
			4 classes	8 classes	3x3	5x5	7x7
	<b>IDM</b>						
1	3x3	86.57	87.43	89.71	90.29	89.43	89.43
2	5x5	81.14	87.43	80.57	88.86	88.57	90.86
3	7x7	78.29	80.86	78.00	86.86	90.57	90.51
4	9x9	77.71	79.14	77.43	86.29	89.14	90.86
5	11x11	79.43	78.00	80.86	79.71	79.50	89.75
6	13x13	81.43	78.28	80.86	79.71	80.50	90.00
7	15x15	81.71	78.57	81.43	79.71	80.75	80.00
8	17x17	84.29	80.86	83.71	83.71	81.71	81.72
9	19x19	86.57	80.86	86.57	83.43	82.57	83.71
10	21x21	88.28	81.71	88.00	84.86	86.00	86.29
11	23x23	88.28	81.43	88.00	86.00	87.71	88.29
12	25x25	88.00	82.00	87.43	88.00	88.00	88.00
	<b>CON</b>						
13	3x3	82.86	87.14	83.71	82.86	89.71	90.00
14	5x5	79.43	87.14	79.71	83.14	86.86	90.57
15	7x7	80.57	85.71	80.27	87.43	87.14	89.43
16	9x9	80.00	86.00	81.71	86.57	86.57	89.14
17	11x11	82.86	86.00	82.57	87.14	85.75	89.75
18	13x13	83.43	85.71	81.14	87.14	85.75	88.50
19	15x15	83.71	86.00	82.86	86.75	87.50	89.00
20	17x17	85.14	87.43	82.29	87.43	88.29	87.71
21	19x19	85.71	87.14	82.00	88.57	88.00	88.57
22	21x21	85.71	86.29	82.86	88.57	87.14	88.86
23	23x23	85.43	86.86	82.58	88.29	86.29	88.86
24	25x25	85.43	86.86	82.29	87.14	87.43	88.29
	<b>ENT</b>						
25	3x3	87.71	88.00	88.86	88.57	89.71	88.86
26	5x5	87.43	85.43	88.57	87.43	89.43	88.57
27	7x7	86.57	85.71	87.71	86.86	90.00	88.86
28	9x9	84.28	86.00	86.00	88.00	88.86	87.71
29	11x11	86.00	86.57	86.00	87.25	88.00	90.25
30	13x13	87.43	86.29	86.29	88.75	89.25	90.50
31	15x15	86.86	86.00	84.86	89.75	89.50	90.75
32	17x17	89.43	87.71	87.43	88.29	89.14	90.00
33	19x19	89.43	86.57	87.43	87.14	89.14	90.00
34	21x21	88.00	86.87	87.43	87.43	88.86	88.29
35	23x23	88.00	87.43	87.43	88.00	89.14	87.43
36	25x25	88.00	89.14	86.86	87.71	90.00	88.00

Table 3. (continue)

No	Image quantization method						
	Texture	the 256 grey level	Segmentation		Averaging filtered		
	Window size		4 classes	8 classes	3x3	5x5	7x7
	<b>ENE</b>						
37	3x3	88.00	87.14	88.57	90.29	89.43	89.14
38	5x5	81.71	86.29	88.00	89.71	88.86	89.14
39	7x7	82.29	84.29	87.14	89.14	88.57	88.86
40	9x9	82.29	86.00	81.14	88.29	89.43	90.29
41	11x11	80.57	86.86	79.43	86.25	89.25	90.00
42	13x13	79.71	86.86	78.57	85.00	89.00	90.00
43	15x15	79.43	87.43	78.29	82.75	88.50	89.25
44	17x17	81.14	88.00	80.86	80.29	82.29	89.14
45	19x19	80.86	86.57	80.86	80.57	81.43	88.29
46	21x21	81.71	86.86	80.57	81.14	80.86	87.71
47	23x23	81.43	86.86	81.14	81.43	81.43	88.00
48	25x25	81.14	86.00	80.29	81.14	81.43	88.00

Note: IDM=inverse difference moment, CON=contrast, ENT=entropy, ENE=energy.

The result also indicates that the increase of number of textural features does not contribute to increases classification accuracy. In case of image segmentation for eight classes, integrated multiple textural of inverse different moment and energy provides highest classification accuracy of 88.75%, which is not significant by different from using single textural feature (Table 4). However, the highest classification accuracy of 91% was achieved when using inverse different moment (5 x 5) and energy (9 x 9) from averaging filtered image with window size of 7x7. Table 5 shows the best overall accuracy of classification results for each image quantization method using single and multiple textural features. Combination of number 3 provides the overall classification result of 91% using integration of spectral and multiple textural features. This combination improved significantly individual classification results of fallow land and residential classes than compared with only using spectral features. Table 6 shows the error matrix of the best classification result.

It can be explained that a pair class of fallow land and residential contributing in mixture of misclassification therefore individual accuracy of these classes were lower than other classes. However these classes have been improved using integration of spectral and textural features, single or multiple features.

Table 4. The overall accuracy of classification results using multiple textural features for image segmentation

No	Data set	Texture	Overall accuracy (%)	
			4 classes	8 classes
1	Using 2 textures	IDM + CON	84.00	81.75
2		IDM + ENT	85.25	86.50
3		IDM + ENE	84.25	88.75
4		CON + ENT	84.25	82.50
5		CON + ENE	85.25	81.50
6		ENT + ENE	85.75	86.25
7	Using 3 textures	IDM + CON + ENT	82.75	80.75
8		IDM + CON + ENE	83.75	82.25
9		IDM + ENT + ENE	83.75	85.75
10		CON + ENT + ENE	84.25	80.25
11	Using 4 textures	IDM + CON + ENT + ENE	83.50	80.50

Table 5. The best overall accuracy of classification results for each image quantization method using single and multiple textural features

No	Image quantization	Texture (window size)		Overall accuracy (%)	
		Single	Multiple	Single	Multiple
1	A 256 grey level image	ENT(17x17)	IDM(21x21) + ENT(17x17)	89.43	85.75
2	Image segmentation (8 classes)	IDM(3x3)	IDM(3x3) + ENE(17x17)	89.71	88.75
3	Averaging filtered (7x7)	IDM(5x5)	IDM(5x5) + ENE(9x9)	90.86	91.00

Table 6. The error matrix of the best classification result using the spectral and textural features

Classified as	Reference data					
	Water	Fallow	Tea	Vegetable	Residential	Total
Water	<b>19</b>	0	0	0	0	19
Fallow	0	<b>74</b>	2	4	5	85
Tea	0	0	<b>59</b>	4	1	64
Vegetable	0	4	2	<b>140</b>	4	150
Residential	0	4	1	5	<b>72</b>	82
<b>Total</b>	19	82	64	153	82	<b>400</b>

The overall accuracy is  $19+74+59+140+72/400 = 91.00\%$

## CONCLUSIONS

From the foregoing discussion, the following conclusions were obtained :

- (1) The use of integrated spectral and textural features approach provide better accuracy compared to the use of the spectral approach only.
- (2) Increase in the size of the window (from 3x3 to 15x15 pixels) improved the overall accuracy up to a certain limit. For all the features, the optimal window size was identified between 5x5, 7x7, and 9x9 pixels.
- (3) Proposed image quantization methods brought the improvement to provide better overall classification accuracies than using a 256 grey level image.

## REFERENCES

- Bandibas, J.C., 1998. Combining the spectral and spatial signatures of information classes using artificial neural network based classifier for remote sensing of spatially heterogeneous land use/land cover systems in tropics. Proceeding of the 19<sup>th</sup> Asian Conference on Remote Sensing. Manila, Philippine, 16-20 November.
- Baraldi, A. and Parmiggiani, F., 1995. An investigation of the textural characteristics associated with grey level cooccurrence matrix statistical parameters. IEEE Transaction on Geoscience and Remote Sensing, 33(2): 293-304.
- Beauchemin, M., Thomson, K.P.B. and Edwards, G., 1996. Edge detection and speckle adaptive filtering for SAR images based on a second-order textural measure. International Journal of Remote Sensing, 17(9): 1751-1759.
- Colby, D., 1991. Topographic normalization in rugged terrain. Photogrammetric Engineering and Remote Sensing, 57(5): 531-537.
- Congalton, R., 1991. A review of assessing the accuracy of classifications of remotely sensed data. Remote Sensing of Environment, 37, 35-46.
- Congalton, R. and Green K., 1999. Assessing the accuracy of remotely sensed data; principles and practices. Lewis Publishers, Boca Raton.
- Connors, R.W., Trivedi, M.M. and Harlow, C.A., 1984. Segmentation of a high-resolution urban scene using texture operators. Computer Vision Graph and Image Processing, 25, 273-310.
- Dutra, L.V. and Nelson, D.A.M., 1984. Some experiments with spatial feature extraction methods in multispectral classification. International Journal of Remote Sensing, 5(2): 303-313.
- Data monografi kecamatan (2001). Kecamatan Pangalengan, Bandung, Jawa Barat.
- Haralick, R. M., Shanmugam, K. and Dinstein, I., 1973. Textural features for image classification. IEEE Transaction Systemic, Man, Cybernetics, SMC-3(6): 610-621.
- Horgan, G.W., Glasbey, C.A., Soria, S.L., Gozalo, J.N.C., and Alonso, F.G., 1992. Land use classification in central Spain using SIR-A and MSS imagery. International Journal of Remote Sensing, 13(15): 2839-2848.

- Jensen, J.R., 1996. Introductory digital image processing; a remote sensing perspective. Prentice Hall Inc., Tokyo
- Karathanassi, V., Iossifidis, C.H. and Rokos, D., 2000. A texture-based classification method for classifying built areas according to their density. *International Journal of Remote Sensing*, 21(9), 1807-1823.
- Kuplich, T.M., Freitas, C.C. and Soares, J.V., 2000. The study of ERS-1 SAR and Landsat TM synergism for land use classification. *International Journal of Remote Sensing*, 21(10): 2101-2111.
- Kurosu, T., Uratsuka, S., Maeno, H. and Kozu, T., 1999. Texture statistics for classification of land use with multitemporal JERS-1 SAR single-look imagery. *IEEE Transaction on Geoscience and Remote Sensing*, 37(1): 227-235.
- Kushwaha, S.P.S., Kuntz, S. and Oesten, G., 1994. Applications of image texture in forest classification. *International Journal of Remote Sensing*, 15(11): 2273-2284.
- Lillesand, T.M. and Kiefer, R.W., 1994. Remote sensing and image interpretation. John Wiley & Sons, Inc., New York.
- Marceau, D.J., Howarth, P.J., Dubois, J.M. and Gratton, D.J., 1990. Evaluation of the grey level co-occurrence matrix method for land cover classification using SPOT. *IEEE Transaction on Geoscience and Remote Sensing*, 28(4): 513-519.
- Ryherd, S. and Woodcock, C., 1996. Combining spectral and texture data in the segmentation of remotely sensed images. *Photogrammetric Engineering and Remote Sensing*, 62(2): 181-193.
- Shaban, M.A. and Dikshit, O., 1999a. Evaluation of merging SPOT multispectral and panchromatic data for classification of urban environment", *Proceeding of International Geoscience and Remote Sensing Symposium (IGARRS)*, Hamburg, Germany, 28 June - 2 July.
- Shaban, M.A. and Dikshit, O., 1999b. Land use classification for urban areas using spatial properties. *Proceeding of International Geoscience and Remote Sensing Symposium (IGARRS)*, Hamburg, Germany, June 28- July 2.
- Smits, P.C., Dellpiane, S.G., Annoni, A. and Ehrlich, D., 1998. Multi-temporal analysis of urban areas using textural information in space-borne imagery. *Proceeding of International Geoscience and Remote Sensing Symposium (IGARRS)*, Seattle, Washington, USA, July 6-10.
- Soares, J.V., Renno, C.D., Formaggio, A.R., Yanasse, F. and Frery, A.C., 1997. An investigation of the selection of texture features for crop discrimination using SAR imagery. *Remote Sensing of Environment*, 59, 234-247.
- Toll, D., 1985. Analysis of digital Landsat-MSS and SEASAT SAR data for use in discriminating land cover at the urban fringe of Denver, Colorado. *International Journal of Remote Sensing*, 6(7): 1209-1229.
- Zhang, Y., 1999. Optimisation of building detection in satellite images by combining multispectral classification and texture filtering. *ISPRS Journal Photogrammetry and Remote Sensing*, 54, 50-60.